Heliyon 9 (2023) e15495

Contents lists available at ScienceDirect

Heliyon

journal homepage: www.cell.com/heliyon

Research article

A new approach to the development and assessment of doxorubicin-loaded nanoliposomes for the treatment of osteosarcoma in 2D and 3D cell culture systems

Mastaneh Parchami [a], Fateme Haghiralsadat [b,c,**], Fatemeh Sadeghian-Nodoushan [b,d], Mahdie Hemati [b,e,*], Sajjad Shahmohammadi [b], Nasrin Ghasemi [f], Ghasem Sargazi [g]

[a] Department of Medical Biotechnology, Faculty of Medicine, Shahid Sadoughi University of Medical Sciences, Yazd, Iran
[b] Medical Nanotechnology and Tissue Engineering Research Center, Yazd Reproductive Sciences Institute, Shahid Sadoughi University of Medical Sciences, Yazd, Iran
[c] Department of Advanced Medical Sciences and Technologies, School of Paramedicine, Shahid Sadoughi University of Medical Sciences, Yazd, Iran
[d] Department of Tissue Engineering and Applied Cell Sciences, School of Advanced Technologies in Medicine, Shahid Beheshti University of Medical Sciences, Tehran, Iran
[e] Department of Clinical Biochemistry, Faculty of Medicine, Shahid Sadoughi University of Medical Sciences, Yazd, Iran
[f] Abortion Research Centre, Yazd Reproductive Sciences Institute, Shahid Sadoughi University of Medical Sciences, Bouali Ave, Safaeyeh, Yazd, Iran
[g] Non-communicable Diseases Research Center, Bam University of Medical Sciences, Bam, Iran

ARTICLE INFO

Keywords:
Osteosarcoma
Saos-2
Nanoliposome
Scaffold
Alginate hydrogel
Doxorubicin

ABSTRACT

Doxorubicin (DOX) is an effective anticancer drug used for the treatment of osteosarcoma. Liposomal nanocarriers for doxorubicin administration are now regarded as one of the most promising approaches to overcome multiple drug resistance and adverse side effects. The use of hydrogel as a 3D scaffold to mimic the cellular environment and provide comparable biological conditions for deeper investigations of cellular processes has attracted considerable attention. This study aimed to evaluate the impact of liposomal doxorubicin on the osteosarcoma cell line in the presence of alginate hydrogel as a three-dimensional scaffold. Different liposomal formulations based on cholesterol, phospholipids, and surfactants containing doxorubicin were developed using the thin-layer hydration approach to improve therapeutic efficacy. The final selected formulation was superficially modified using DSPE-mPEG2000. A three-dimensional hydrogel culture model with appropriate structure and porosity was synthesized using sodium alginate and calcium chloride as crosslinks for hydrogel. Then, the physical properties of liposomal formulations, such as mechanical and porosity, were characterized. The toxicity of the synthesized hydrogel was also assessed. Afterward, the cytotoxicity of nanoliposomes was analyzed on the Saos-2 and HFF cell lines in the presence of a three-dimensional alginate scaffold using the MTT assay. The results indicated that the encapsulation efficiency, the amount of doxorubicin released within 8 h, the mean size of vesicles, and the surface charge were 82.2%, 33.0%, 86.8 nm, and

* Corresponding author. Medical Nanotechnology and Tissue Engineering Research Center, Yazd Reproductive Sciences Institute, Shahid Sadoughi University of Medical Sciences, Yazd, Iran.Tel.: +09135140586.
** Corresponding author. Medical Nanotechnology and Tissue Engineering Research Center, Yazd Reproductive Sciences Institute, Shahid Sadoughi University of Medical Sciences, Yazd, Iran. Tel.: +989132507158.
E-mail addresses: mparchami_90@yahoo.com (M. Parchami), fhaghirosadat@gmail.com (F. Haghiralsadat), m.hemati1420@gmail.com (M. Hemati).

https://doi.org/10.1016/j.heliyon.2023.e15495
Received 22 October 2022; Received in revised form 29 March 2023; Accepted 11 April 2023
Available online 20 April 2023

−4.2 mv, respectively. As a result, the hydrogel scaffolds showed sufficient mechanical resistance and suitable porosity. The MTT assay demonstrated that the synthesized scaffold had no cytotoxicity against cells, while nanoliposomal DOX exhibited marked toxicity against the Saos-2 cell line in the 3D culture medium of alginate hydrogel compared to the free drug in the 2D culture medium. Our research showed that the 3D culture model physically resembles the cellular matrix, and nanoliposomal DOX with proper size could easily penetrate into cells and cause higher cytotoxicity compared to the 2D cell culture.

Abbreviations

DOX	Doxorubicin
Chol	Cholesterol
SPC80	Soybean phospholipids with (75% phosphatidylcholine)
DSPE-mPEG 2000	1,2-distearoyl-*sn*-glycero-3- phosphoethanolamine-*N*-[methoxy (polyethylene glycol)-2000
DOPE	1,2-dioleoyl-*sn*-glycero-3-phosphoethanolamine
L/D	Lipid/Drug ratio
Lipo-DOX	Liposomal DOX
PBS	Phosphate-buffered saline
DMSO	Dimethyl sulfoxide
MTT	3-(4,5-dimethyl-2-thiazolyl)-2,5-diphenyl2-H-tetrazolium bromide
Dil	1,1′-Dioctadecyl-3,3,3′,3′-Tetramethylindocarbocyanine Perchlorate
DAPI	4′,6-diamidino-2-phenylindole
2D	Two Dimensional
3D	Three Dimensional
EE%	Encapsulation Efficiency
DL%	Drug Loading
DLS	Dynamic Laser Scattering
PDI	Polydispersity Index
SEM	Scanning Electron Microscope
FTIR	Fourier transform infrared
XRD	X-ray powder diffraction

1. Introduction

Osteosarcoma (OS) is the third leading cause of cancer in adolescents and is more prevalent in men. Only 10% of patients are over 60 years old, and over 60% of patients are between the ages of 15 and 20 [1,2]. It is a mesenchymal-derived invasive malignant neoplasm that often originates in bone but may also occur in soft tissue [3]. Treatment of osteosarcoma depends on various factors, such as the extent of malignancy, the stage, and location of cancer, as well as the age and general health of patients. The major therapies for this type of cancer include surgery, chemotherapy, and radiation. Osteosarcoma is usually treated with chemotherapy for approximately 10 weeks before surgery and again for up to a year following surgery [4]. Doxorubicin (DOX) is a chemotherapeutic agent used for the treatment of osteosarcoma alone or in combination with one or more other drugs, such as cisplatin [5]. DOX is a non-selective anthracycline drug employed for the treatment of lung cancer, breast cancer, gastric cancer, and other types of malignancies [6,7]. Doxorubicin binds to DNA-related enzymes and can intercalate into the base pairs of double-stranded DNA. This medicine, like other anthracyclines, inhibits the function of Topoisomerase II, an enzyme required for the growth of cancer cells, by interfering with the Topo II-DNA complex during the replication process with its sugar components and cyclohexane ring A [8]. The use of this drug also has limitations, the most important of which is its cardiac toxicity [9]. Due to its non-selective nature, doxorubicin also affects normal cells, such as immunological cells, hence weakening the patient's immune system and increasing vulnerability to infectious infections [10]. In order to decrease the toxicity of the medicine and its side effects, notably in the field of chemotherapy, it has become crucial to design drug delivery systems that employ pharmaceuticals with a precise concentration and duration in a targeted location [11]. A number of drug delivery systems have been designed and utilized, and liposomes are one of the most common systems used for the targeted delivery of drugs. Liposomes are being employed to enhance therapeutic indicators by improving absorption, decreasing metabolism, increasing the half-life, and decreasing the side effects and toxicity of drugs [12]. The advantages and disadvantages of these nanocarriers are dependent on their physical and chemical properties, such as their size, composition, stability, and biological interactions with the cell membrane. Liposomes are capable of effectively encapsulating both hydrophilic and hydrophobic substances. Because of their biocompatibility and degradability, they are particularly significant drug carriers [13,14]. Despite their advantages, liposomes have disadvantages, including physical instability, degradation of phospholipids, rapid clearance

by the immune system from the circulation, and premature leakage of bioactive compounds from vesicles. Several studies have been performed to overcome these challenges. A new PEGylated liposomal DOX composition was rationally designed in the current research to overcome these constraints associated with liposomes. The optimal molar ratio mixture of phospholipids and surfactants with suitable entrapment effect, release behavior, and stable properties provide an excellent solution for DOX encapsulation. Surfactants in the formulation of liposomes reduce the particle size and improve the encapsulation efficiency and release properties of liposomes by reducing the surface tension and stabilizing the interface between aqueous and non-aqueous vesicles [15,16]. DOPE acts as an auxiliary lipid and fusion in the structure of liposomes. It facilitates membrane fusion, which increases the efficient delivery of DOX to the target site. The flow cytometry analysis showed a much higher fusion efficiency in the case of DOPE-containing liposomes [17]. On the other hand, the addition of DOPE to the acidic tumor environment increased the regulated release of DOX in tumors [18]. In this research, polyethylene glycol (PEG, 2000) was used to increase the circulation time of the drug, reduce the absorption of the reticuloendothelial system, and inhibit the clearance of liposomes from the immune system [19]. Thus, these efficient modification routes in the liposome structure were proved in stabilizing liposomes with high encapsulation efficiency and controversial release of DOX. To better understand the impact of the extracellular environment, different chemicals, and medications on cells, synthetic materials, particularly hydrogels, have drawn the interest of researchers in recent years. These materials are used to demonstrate more precise and realistic cell responses. On the other hand, hydrogel scaffolds create a three-dimensional structure that is more similar to natural tissue. As a result, cells have more flexibility for growth and differentiation on hydrogel scaffolds. For this reason, its use in the fields of biomedicine and pharmaceutical research has made significant progress in recent years [20]. Hydrogels are three-dimensional polymers absorbing significant amounts of water and biofluids because their polymer chains include hydrophilic functional groups [21]. This polymeric network is sensitive to environmental stimuli (ions, pH, temperature, enzyme presence, electric field) and, therefore, can swell or shrink [22]. The porosity of these scaffolds, on the other hand, facilitates permeability and material exchange. Hydrogels also have benefits in terms of biocompatibility, biodegradability, and injectability [23,24]. These characteristics make hydrogels useful agents for industry, agriculture, controlled release systems, and medical applications. Hydrogels can be prepared using two groups of natural and synthetic polymers. Alginate is the most widely used natural polymer in their construction [25]. Alginate is a natural polysaccharide usually extracted from brown algae and consists of linear copolymers of β-D mannuronic acid and α-L-guluronic acid units. Due to variations in the quantity and sequence of monomer dispersion, this polymer displays an irregular organization [26,27]. The mechanical strength of alginate hydrogels varies depending on the cation's affinity to alginate. Depending on the technique of crosslinking, drug molecules, tiny compounds, or macromolecular proteins may be released from alginate gels in a regulated manner. Besides, alginate gels could be injected orally or in a minimally invasive manner, allowing for widespread use for biomedical purposes. In cell culture, the absence of mammalian cell receptors for alginates, along with the low rate of protein uptake, enables them to serve as an ideal blank plate for the application of extremely specific cell adhesion mechanisms [26]. Alginate is widely used in tissue engineering, cell culture, and drug delivery because of its optimum properties, such as biocompatibility and non-toxicity, suitability for cell proliferation and adhesion, antibacterial nature, and biodegradable activities [28,29]. The present study aims to

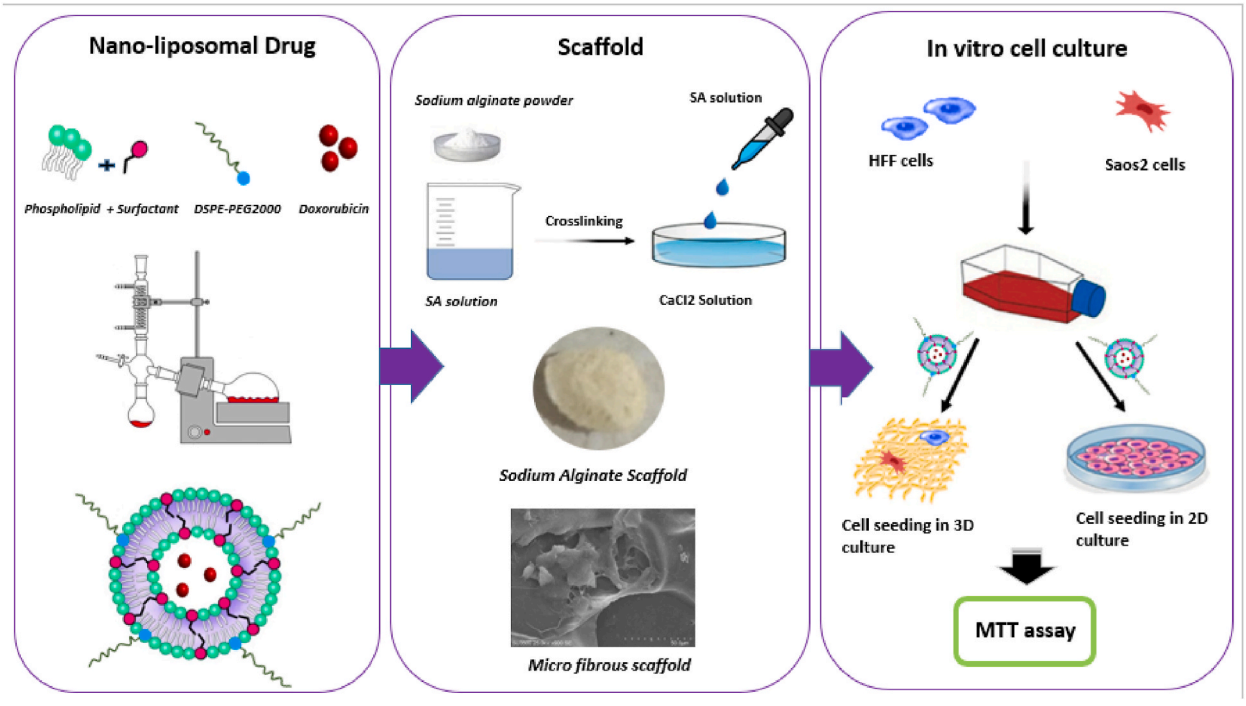

Fig. 1. Graphical abstract.

develop and characterize a new formulation of Lipo-DOX and alginate hydrogels as 3D scaffolds with an approach to improve stability and non-aggregation behavior and our ability to control the performance of encapsulated DOX in delivery applications. Then the effects of optimal nanoliposome DOX on the osteosarcoma cell line and HFF as a normal cell line were investigated, and its cytotoxicity was compared in 2D tissue culture plates and 3D hydrogel scaffold as an engineered tumor model (Fig. 1).

2. Materials and methods

2.1. Chemicals

Doxorubicin HCl (DOX) was obtained from Cell Pharm (Germany). Tween-60 and Tween-80 were purchased from Merck (Darmstadt, Germany). Distearoyl phosphoethanolamine, polyethylene glycol (Lipoid PE 18: 0/18: 0 – PEG2000, DSPEmPEG 2000), 1,2-dioleoyl-*sn*-glycero-3-phosphoethanolamine (DOPE) and SPC80 (soybean phospholipids with 75% phosphatidylcholine were obtained from Lipoid GmbH (Ludwigshafen, Germany). Cholesterol and sodium alginate were supplied by Sigma-Aldrich (St. Louis, MO, USA). PBS (Phosphate-buffered saline) tablets, dialysis bag (MW 12–14 kDa), DMSO (dimethyl sulfoxide), HEPES buffer, MTT (3-(4,5-dimethylthiazol-2-yl)-2,5-diphenyl tetrazolium bromide) and paraformaldehyde solution were procured from Sigma-Aldrich (St. Louis, MO, USA). DAPI (40,6-diamidino- 2-phenylindole) was supplied from Thermo Fisher Scientific (Massachusetts, USA). All other chemicals, solvents, and salts were of the analytical grade and used without further purification unless specified.

2.2. Preparation of doxorubicin-loaded nanoliposomes (Lipo-DOX)

The thin film method was used for the preparation of liposomal DOX. In brief, cholesterol, SPC, DOPE, DSPE-PEG2000, Tween-60, and Tween-80 were dissolved in chloroform and evaporated at 45 °C in different formulations and mole ratios with Lipid/Drug (L/D) 10. Also, to evaluate the cellular internalization of Lipo-DOX, fluorescent dye Dil (Sigma, USA) was added at 0.1 mol% for lipid staining. The thin lipid film was hydrated at a certain volume of DOX (500 μg/ml concentration) and dissolved in PBS at 50 °C for 60 min using a rotary instrument (Heidolph, Germany). Multilamellar formed vesicles (MLVs) were sonicated to produce small unilamellar vesicles (SUVs) for 60 min using a microtip probe sonicator (E–Chrom Tech Co, Taiwan) equipped with a micro tip with a diameter of 5 mm and a power of 60 W inside an ice bath. Subsequently, small unilamellar vesicles (SUVs) were dialyzed against PBS to separate the unloaded DOX from Lipo-DOX.

2.3. Preparation of sodium alginate hydrogel (scaffold)

In order to produce hydrogel scaffolds, 1% (w/v) sodium alginate powder (120,000 g/mol) was dissolved in distilled water and stirred for 3 h at room temperature. After that, 300 μl of alginate solution was added to 500 μl of calcium chloride solution (3% w/v), incubated at 37 °C for 15 min, and stored at −20 °C. After 1 h, calcium chloride was discarded, and then the Emulsion Freeze Drying method was used to create suitable porosity in the gel for 48 h. The freeze-drying technique is suitable for various types of hydrogel materials, including natural and synthetic hydrophilic polymers, to fabricate interconnected porous structures. Briefly, the emulsion mixture of polymer, solvent, and non-solvent is exposed to liquid nitrogen and quenched at low temperatures [30,31].

2.4. Characterization of Lipo-DOX and sodium alginate scaffold

2.4.1. Entrapment efficiency and in-vitro drug release assay of Lipo-DOX.

DOX-loaded nanoliposomes were placed in a dialysis cellulose membrane to remove the non-encapsulated drugs (cut-off = 12–14 kDa). Spectroscopic measurements were used to assess the encapsulation efficiency. After lysing with isopropanol (99% purity), the quantities of DOX loaded into nanoparticles were determined using the UV-spectrophotometry method at 480 nm. The encapsulation efficiency (EE%) (equation (1)) and drug loading (DL%) (equation (2)) were calculated using the following formula:

$$Entrapment\ Efficiency\ (\%EE) = \frac{Encapsulated\ Drug\ Concentration\ \left(\frac{mg}{ml}\right)}{Primary\ used\ Drug\ Concentration\ \left(\frac{mg}{ml}\right)} \times 100 \tag{1}$$

$$Drug\ Loading\ (DL\%) = \frac{mass\ of\ encapsulated\ DOX\ (mg)}{mass\ of\ liposomes\ (mg)} \times 100 \tag{2}$$

in order to assay the release profile of Lipo-DOX, 500 μl of the nanoliposomal doxorubicin was transferred into the dialysis bag with a cut-off value of 12 kDa and while a 0.5-cm magnet was connected to its end. The dialysis bag was incubated in tube falcons containing 10 ml of the release medium (PBS; pH 7.4). The tube falcons were then submerged in beaker water and placed on a heater stirrer with continual magnetic stirring at 75 rpm for 72 h. The temperature of the heater stirrer was set at 37 °C and 42 °C (simulating the tumor microenvironment) [32–34]. In order to determine the quantity of DOX released, the medium of samples obtained at various intervals was replaced with fresh PBS and then recalculated. DOX was evaluated in samples using UV spectrophotometry at 480 nm.

2.4.2. Particle size and zeta potential of Lipo-DOX

The surface charge of the synthesized nanoliposome (Z-average), the hydrodynamic size diameter based on the z-average and

polydispersity index (PDI) was measured by a ZetaSizer instrument (Horiba SZ-100, Horiba Mfg. Co. Ltd, Kyoto, Japan).

2.4.3. Morphological and structural analysis of Lipo-DOX and hydrogel scaffold

The atomic force microscope (AFM) (Ara research, Noncontact, Iran) analysis was used to evaluate the surface properties of nanoliposomes. To this aim, samples were sonicated for 10 min, and then a small thin film of the pellet was prepared and placed on a glass slide. Finally, the prepared samples were imaged using AFM.

The surface morphology of liposome-containing DOX was analyzed using scanning electron microscopy (SEM) (model KYKY-EM3200, KYKY, Beijing, China). For this purpose, the samples were placed on a glass plate and covered with a gold coating for 300 s at a voltage of 20 kV to make them conductive. Also, the morphology and microstructure of the sodium alginate hydrogel, following the freeze-drying process, were analyzed by SEM. Afterward, the freeze-dried samples were completely dehydrated with ethanol, mounted on aluminum stubs, sputter-coated with gold finally analyzed using SEM.

2.4.4. Functional group characterization

The functional groups and surface characterization of free DOX, blank liposome, Lipo-DOX, and sodium alginate scaffold, as well as molecular interaction between DOX and liposome components, were investigated using FTIR spectroscopy (AVATAR, Thermo, USA). Samples were prepared as dry powders and mixed separately with potassium bromide (KBr), and pressed into the pellets.

2.4.5. X-ray diffraction (XRD)

The X-diffraction patterns of the sodium alginate scaffold were obtained using Philips (Holland) PW1730 diffractometer. The wavelength of the radiation was 1.54056 Å at a voltage of 40 kV and a current of 30 mA. XRD pattern for sodium alginate was obtained by scanning from 0° to 80° (2θ).

2.4.6. Mechanical test

The compressive modulus of the hydrogel was evaluated using the universal testing equipment to assess its mechanical characteristics (Zwick/Roell Z020). In this experiment, all hydrogels were prepared in the form of cylinders (10 mm in diameter and 10 mm in height) and were subjected to compression at a rate of 0.5 mm/min until the destruction of hydrogels. The results have been reported in the form of a force diagram in terms of the percentage of compressive strain.

2.4.7. Porosity measurements

The liquid displacement technique was used to measure the porosity of scaffolds. First, some ethanol was put into the falcon and weighed to determine the porosity of the scaffolds. The falcons were then placed on the shaker while freeze-dried scaffolds of the same weight were poured into ethanol. After 4 h, the scaffolds were removed, the falcon containing ethanol was weighed, and the porosity % of the scaffolds was estimated using the following formula (equation (3)):

$$\%\ Porosity = \frac{(w2 - w3 - ws)}{(w1 - w3)} \times 100 \tag{3}$$

$$W1 = Falcon\ weight + Ethanol\ weight$$

$$W2 = Ethanol\ weight + Hydrogel\ weight$$

$$W3 = The\ weight\ of\ ethanol\ after\ removing\ the\ hydrogel$$

$$Ws = Dry\ weight\ of\ the\ hydrogel$$

2.5. Cell culture

The human foreskin fibroblast (HFF) cell line was obtained from Medical Nanotechnology and Tissue Engineering Research Center (Yazd, Iran). The human osteosarcoma cell line, Saos-2, was purchased from the Pasteur Institute of Iran (Tehran, Iran). All cells were cultured in DMEM (Gibco, Grand Island, NY) supplemented with penicillin–streptomycin (Gibco, Grand Island, NY) and 10% fetal bovine serum (FBS) (Gibco, Grand Island, NY) under standard conditions (37 °C and 5% CO_2 in a humidified incubator).

2.5.1. In-vitro evaluation of cellular uptake

The fluorescence intensity of DOX was measured to assess the distribution of DOX in the nucleus. In brief, Saos-2 and HFF cells (10^5 cells per well) were seeded onto 6-well plates and subsequently treated with 10 μg/ml free DOX, Lipo-DOX and blank liposome. The fluorescent 1,1′-dioctadecyl-3,3,3′,3′-tetramethylindocarbocyanine (DiI) dye was utilized in liposome manufacturing to assess the delivery efficiency and cellular uptake of blank liposomes. After 3 h, all the floating cells were removed and washed thrice with PBS (pH = 7.4). DAPI (1 mg/ml) was used as a counterstain for the nucleus of cells for 15 min. Fluorescent microscopy images were taken using an Olympus fluorescence microscope with a 60× magnification, UV (blue), and Texas (red) filters for DAPI (358 nm) and DOX (561 nm), respectively, as the excitation source.

2.5.2. Cytotoxicity assay

2.5.2.1. 2D culture. In order to investigate the cellular anti-proliferative activity of free DOX and Lipo-DOX at various concentrations (1.25, 2.5, 5, 7.5, 10, 15 μg/ml), the compounds were incubated for 48 h with 10^4 cells in a 96-well plate and evaluated using the colorimetric MTT assay. The control wells and samples were rinsed with PBS after 48 h of cell seeding in the cell culture medium and then incubated for 3 h with 20 μl of 5 mg/ml MTT in PBS. The resulting formazan crystals were dissolved in DMSO. The absorbance of the obtained samples was measured using a microplate reader (Synergy HTX, Bio-Tek, Winooski, VT) at a wavelength of 570 nm.

2.5.2.2. 3D culture. First, the MTT assay was performed to measure the cytotoxic activity of the alginate scaffold for 1, 3, and 7 days. Then, the cytotoxicity of free DOX and Lipo-DOX on cancer and normal cells in the presence of scaffolds was evaluated. Next, 300 μl of sodium alginate (1% w/v) was added to 500 μl of the calcium chloride solution (3% w/v) in each well, incubated at 37 °C for 15 min and kept at −20 °C. After 1 h, the calcium chloride was removed. The plate was freeze-dried, and then the synthesized scaffolds were sterilized using UV light. Then 2×10^4 cells were added to the scaffold and incubated at 37 °C for 24 h. Afterward, the cell culture media were discarded, and the cells were treated with various concentrations (1.25, 2.5, 5, 7.5, 10, 15 μg/ml) of free DOX, Lipo-DOX, and blank liposomes. After 48 h, the cells were harvested, washed with PBS, and incubated with the MTT solution at 37 °C for 3 h. Finally, the DMSO solution was added to dissolve formazan crystals, and the absorbance was recorded at a wavelength of 570 nm.

2.6. Statistical analysis

Graphpad Prism software version 9 (Graphpad, San Diego, CA) was applied for the statistical analysis. Quantitative data were performed in triplicates. The experimental measurements were reported as the mean and standard deviation (mean ± SD). The difference between the groups was analyzed using one-way analysis of variance (ANOVA) followed by Tukey's post hoc test. A p-value of less than 0.05 was considered statistically significant.

3. Results

3.1. Characterization and selection of optimum liposomal formulation

Different liposomal DOX formulations were assessed in order to choose the best formulation in terms of high entrapment efficiency, continuous-release, small size, and zeta potential of vesicles (Table 1). The comparison of phospholipids used in different formulations (F1 vs. F2), consisting of SPC and DOPE, showed that formulation F2 (cholesterol: DOPE) had higher entrapment efficiency and smaller size. However, the high explosive release in the early hours led to the abandonment of this formula; thus, formula F1 was selected. Then, to improve the physicochemical properties of liposomal DOX formulation, the effect of Tween-60 and Tween-80 surfactants on the entrapment efficiency, release, size, and charge of nanoliposomes were investigated. A comparison of two surfactants exhibited that the F3 formula was superior to F4 in terms of physicochemical features. The zeta potential and size of all formulations ranged from - 0.2 to −32 and 86–188 nm, respectively. Finally, 5% DSPE-mPEG (2000) was added to the optimal formulation to generate liposomes with smaller size, less aggregation, longer half-life, and higher stability [35]. In addition, to create spherical liposomal structures, dioleoyl phosphatidyl ethanolamine (DOPE) was employed in the final formula. The formulation F5, Chol: SPC: DOPE: Tween-60: DSPE-PEG2000 was chosen as the optimal formulation for future research due to its high entrapment efficiency, proper release (33% at 8 h), lower diameter 86.8 nm, and PDI less than 0.3.

3.2. In-vitro DOX release assay

Fig. 2 depicts the in-vitro release of DOX from nanoliposomes over 72 h in PBS buffer at pH 7.4 at 37 °C and 42 °C to mimic the temperature of the normal and malignant tissue microenvironments, respectively. The DOX release diagram after 72 h exhibited an early burst followed by a sustained and linear release phase. DOX showed continuous release throughout the release period owing to

Table 1
The effect of various types of lipids on EE%, DL%, short and long-term release, size, zeta potential, and PDI.

Formula	Type of lipids	Lipids (molar ratio%)	Size (nm)	PDI	Zeta potential (mV)	EE %	DL %	% Release (8 h)	% Release (24 h)	% Release (48 h)	% Release (72 h)
F1	Chol: SPC	25:75	169.5	0.394	- 22.1	56.3	5.1	26.6	28.7	28.5	27.6
F2	Chol: DOPE	25:75	131.9	0.089	- 0.2	69.8	6.6	48.1	56.7	65.9	78.5
F3	Chol: SPC: Tween-60	20:60: 20	123.5	0.135	- 14.8	92.6	7.1	22.9	26.2	24.8	23.7
F4	Chol: SPC: Tween-80	20:60: 20	187.9	0.185	- 31.1	68.5	5.2	24.9	29.4	28.0	26.3
F5	Chol: SPC: DOPE: Tween-60: DSPE-PEG2000	12.5:37.5:25: 20:5	86.8	0.254	- 4.2	82.2	5.5	33.0	38.5	39.7	38.2

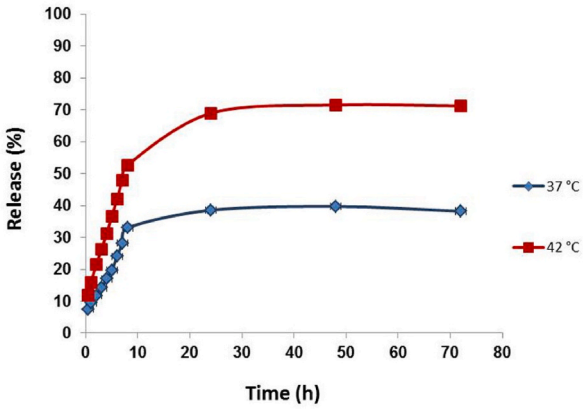

Fig. 2. The drug release profile of Lipo-Dox at 37 °C and 42 °C.

the presence of DSPE-PEG2000 in the liposome structure. The release rates at 37 °C and 42 °C were 38% and 71% after 72 h, respectively. The findings revealed that the release rate increased at higher temperatures; similar to the temperature of the tumor tissue environment, and that its steady pattern is favourable for cancer cells.

3.3. Characterization of optimized formula

3.3.1. Morphological characterization

The size and the morphology of blank liposome and Lipo-DOX were measured by AFM analysis (Fig. 3 A and **B**). The results of AFM were consistent with the findings of the DLS analysis. AFM images depicted that the vesicles size was increased in DOX-loaded vesicles. Fig. 4A depicts the SEM micrographs of Lipo-DOX, demonstrating that all nanoliposomes have a smooth surface, spherical morphology, and well-defined rigid borders. Furthermore, DLS revealed that the diameter of all nanoliposomes was less than 200 nm. The morphology and porosity of the blank scaffold and cell-seeded scaffold are demonstrated in the scanning electron microscopic analysis (Fig. 4 B&C). This Figure demonstrates that the 3D sodium alginate scaffold has a unique and acceptable porosity structure required for cell adhesion. The cells adhered normally to the 3D scaffold and displayed normal morphology, further supporting the suitability and adaptability of the scaffold, as shown in the SEM images. The compound exhibits a homogeneous morphology and is devoid of any aggregation.

3.3.2. FTIR spectral evaluation

The FTIR spectra were analyzed in order to determine the chemical interactions between the components of the liposome and DOX, as well as the functional group Lipo-DOX and blank liposomes. As shown in Fig. 5A, the spectrum of a blank liposome exhibited the distinct peaks of SPC, DOPE, Tween-60, cholesterol, and DSPE-PEG2000 in the range of 3400–1083.98 cm^{-1}, which can be attributed to stretching and bending vibration of hydroxyl bands (band at 3400 cm^{-1}), -CH3 asymmetric and symmetric stretching (2923 cm^{-1}), and -CH2 group asymmetric and symmetric stretching vibration (2853.5 cm^{-1}). The presence of peaks at 1735.8 cm^{-1} and 1460.7 cm^{-1} is attributed to ester group stretching and – CH_2 bending in lipids, respectively. The absorption peaks at 1352.2 cm^{-1} and 1220.6

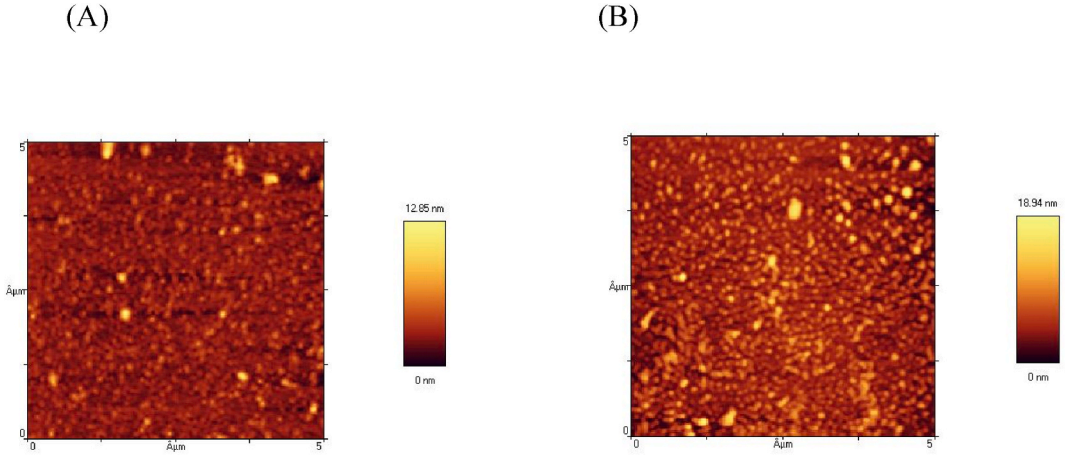

Fig. 3. Atomic force microscopic (AFM) images of the blank (A) and DOX-loaded nanoliposomes (B).

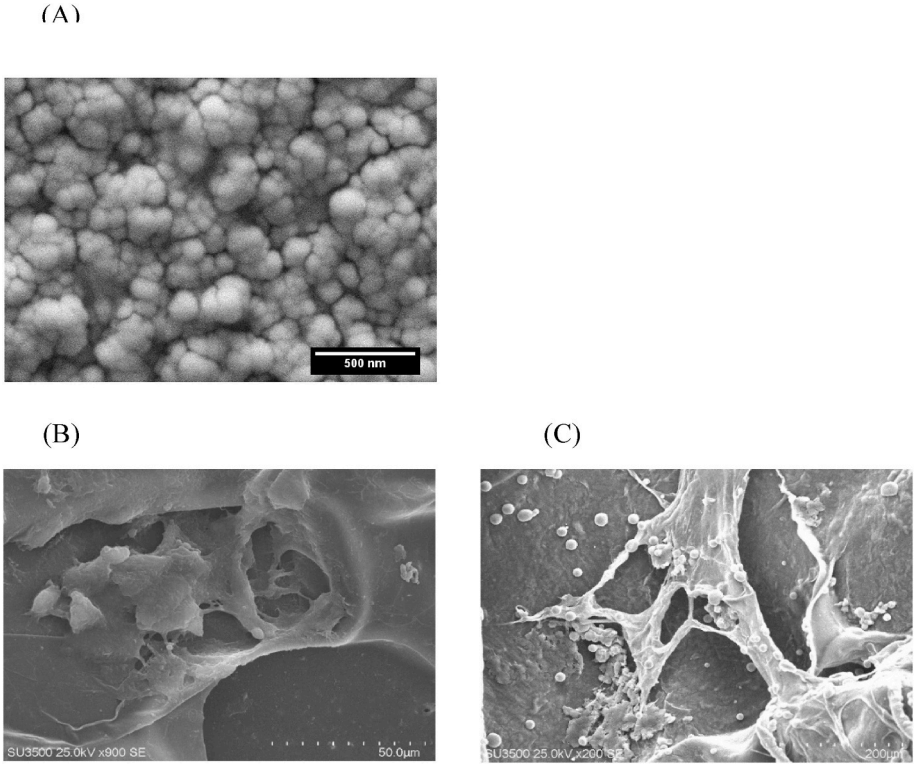

Fig. 4. Scanning electron microscopy (SEM) of DOX-loaded nanoliposomes (A), blank sodium alginate scaffold (B), and sodium alginate scaffolds containing cells (C).

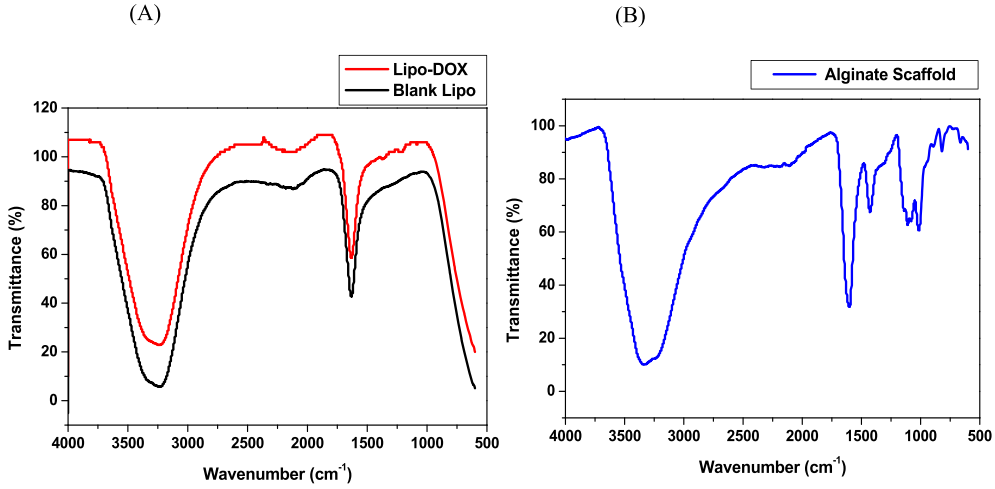

Fig. 5. FTIR spectra of blank liposomes and Lipo- DOX (A), and alginate scaffold (B).

cm^{-1} can be assigned to alkane C–H and alkyl C–N stretching vibration in SPC, DOPE, and DSPE-PEG, respectively. A peak observed at 1083.1 cm^{-1} corresponds to the stretching vibration of ether and ester groups in Tween-60 and DSPE-mPEG. All peaks were repeated in Lipo-DOX. The structural changes in sodium alginate hydrogel were confirmed by FTIR spectroscopy. The obtained spectrum for sodium alginate and its characteristic peaks are shown in Fig. 5B, displaying that the absorption bands at 1601 cm^{-1}, 1427 cm^{-1}, and 1108 cm^{-1} could be assigned to stretching vibrations of asymmetric and symmetric bands of carboxylate anions (-COO), respectively. A peak exhibited in 3342 cm^{-1} corresponds to the hydroxyl group (-OH).

3.3.3. XRD analysis

Fig. 6 depicts the X-ray diffraction pattern of sodium alginate. Sodium alginate has a typical crystalline index of 19.2° and 31.9°, both of which have been described in the literature (26, 27). This pattern suggests that the structure of sodium alginate is retained following fabrication.

3.3.4. Mechanical analysis and porosity measurement of sodium alginate hydrogels

Fig. 7 shows force-deflection graphs of the alginate scaffold under lateral compression that exhibit nonlinear behavior. A curvilinear pattern with low stiffness up to 4 mm deflection was followed by a high stiffness pattern. As the stiffness increased and the stent entirely folded, the force value increased up to 4 mm deflection. The porosity test results showed that the produced sodium alginate scaffold has 68.33 3.51% porosity. These pore sizes with exceptional mechanical properties were appropriate for cell ingrowth.

3.4. Cellular uptake assay

The cellular uptake data show that the blank liposomes may enter the cells effectively. Fig. 8 depicts and compares free and liposomal DOX in Saos-2 and HFF cell lines. As displayed in Fig. 8A, cells treated with liposomal DOX had more purple and turquoise blue color intensity than cells treated with free DOX. The findings showed that the drug encapsulated in liposomal formulation had improved transfection effectiveness owing to its nanoscale and thermosensitive features, which may augment the pharmacological effects of anticancer medications. Furthermore, as demonstrated in Fig. 8B, liposomal DOX showed less penetration into HFF cells than free DOX.

3.5. Antitumor effect of free DOX and Lipo-DOX in 2D and 3D culture systems

The MTT assay was used to assess the cell viability of HFF and Saos-2 cells in the presence of free DOX and Lipo-DOX for 48 h. Lipo-DOX showed increased cytotoxic activity at all concentrations against Saos-2 cells since the liposomal formulation is sensitive to the high temperature of malignant cells (Fig. 9A). However, Lipo-DOX had higher viability efficacy in HFF cells than the free drug, as exhibited in Fig. 9B. The controlled release rate of the liposomal formulation might explain this finding. In addition, the MTT assay was performed in the presence of sodium alginate scaffolds to evaluate the effect of the scaffold on doxorubicin toxicity and to compare 2D and 3D cell culture systems (Fig. 9). As shown in Fig. 9C, the toxicity of the scaffold was investigated after 1, 3, and 7 days and compared with the control cells. The findings showed that the cells placed on the scaffold grew effectively after 7 days. These findings demonstrated that the synthetic scaffold does not cause any harm to the cells and does not impede the normal proliferation of the cells. In cytotoxicity studies performed on HFF cells, it was discovered that liposomal DOX has a slow release rate; as a consequence, it inhibits growth to a lesser extent than free doxorubicin. When compared to 2D cell culture, the cytotoxic capability of Lipo-DOX in Saos-2 cells was dramatically increased when the cell culture was carried out in the presence of sodium alginate scaffolds. This outcome may be explained by the porous structure of the scaffold, which offers an environment for the cells in-vitro that is comparable to the original cell microenvironment.

4. Discussion

Nowadays, most scientists and cancer biologists still apply 2D cell cultures to study the effects of drugs, especially anti-cancer drugs, because of their low-cost and convenience. Considering that cells grown in 2D cell cultures cannot have cell-cell and extracellular matrix interactions like cells in 3D conditions in the body, 2D cell culture cannot be used to accurately display cellular responses to drugs. The use of animal models also has problems, such as high cost, differences in immune system responses in different species, and limited availability [36]. As a result, 3D cell culture systems have been created to offer cellular environmental conditions for biological and pharmacological research on a smaller scale in order to address these challenges. The 3D culture systems simulate the in-vivo and tumor microenvironment in in-vitro conditions, allowing the cells to have cell-cell and cell-matrix interactions. Due to

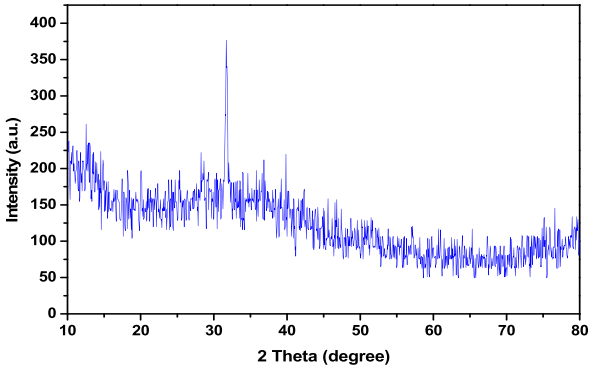

Fig. 6. The X-ray diffraction pattern of sodium alginate scaffold.

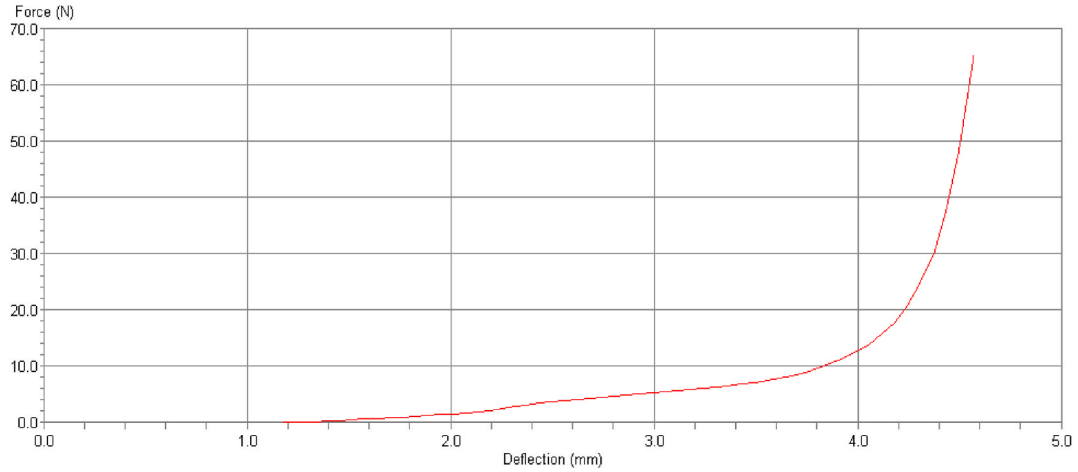

Fig. 7. Mechanical analysis of sodium alginate scaffold; deflection vs. force under lateral compression.

the recognized properties of alginate hydrogel, such as its ability to absorb fluids, nontoxicity, and biocompatibility, we developed an alginate hydrogel scaffold as a 3D cell culture in the current study [37]. Alginate is a biocompatible polysaccharide extensively used as a scaffold due to its rapid gelation in calcium chloride and its high flexibility for encapsulating cells and growth factors, as well as genes and drug delivery [38,39]. A scaffold must have sufficient mechanical resistance to withstand mechanical stress inside the body. When utilized as an implant material for bone reconstruction and supporting newly produced bone tissues, the scaffold must be able to withstand the weight of these tissues. As a consequence, the scaffold uniaxial compression method was utilized to evaluate the mechanical strength of the scaffold, and the findings revealed that our synthesized scaffold displayed great stretching ability and toughness. Average pore size is another characteristic that is considered a determining parameter for tissue engineering scaffolds. In this regard, if the pore size is too small, it becomes difficult for cells to migrate through the scaffold. This feature also prevents nutrient distribution and waste disposal. Conversely, if the pore size is too large, the available surface area for cell adhesion will be limited. In the drying process as a defrosting method, the scaffold pores are formed as ice crystals and grow between the polymer chains. Such a heat-induced phase separation mechanism determines the pore size based on the drying and sublimation of the ice crystal. The result of the porosity test indicated that synthesized alginate hydrogel had 68% porosity which was appropriate for cell implantation and growth. The cytotoxicity of DOX in both free and liposomal forms on osteosarcoma and normal fibroblast cells at 2D and 3D scaffolds was tested and compared in the second phase. We used a nanoliposomal drug delivery system with appropriate nano-scale size, high encapsulation effectiveness, and gradual release to decrease the cytotoxic effects of DOX on normal cells and increase its stability. As a result, new liposome formulations were created utilizing a thin film hydration method. Cholesterol is a neutral fat that is a major component of cell membranes and plays a vital function in their fluidity [40]. The goal of this work was to create a nanoliposome with the smallest size and the best encapsulation efficiency. As a result, we optimized the nanoliposomal DOX with 75% phospholipid and 25% cholesterol, which is the recommended molar ratio based on relevant publications [41]. In order to promote drug penetration, manage drug release, and make nanoliposome vesicles more stable and biocompatible, 25% cholesterol was added to all formulations. Bayindir et al. discovered that cholesterol changes the flexibility of lipid chains and increases the degree of orientational order, thereby decreasing permeability. Furthermore, we employed SPC to design the optimal nanoliposomes [42]. SPC is a natural phospholipid with a structure comparable to biomembrane phospholipids. As a result, it is often used in a variety of drug carriers. Additionally, the unsaturated alkyl chain in SPC increased the flexibility of binding in nanoliposome membranes [43]. Tween-60 was employed in our ideal recipe because its hydrophilic end is important in higher DOX entrapment, as documented in a study carried out by Taymouri et al. [44]. Similar results were reported by Basiri et al. [45]. They represented that the proper ratio of surfactants increased the membrane rigidity and decreased the permeability. Thus, the selected formulation provided the optimal condition for the drug encapsulation and its sustained release properties (Bayindir & Yuksel, 2010). Although the hydrophilic and hydrophobic portions of Tween-60 and Tween-80 were identical, Tween-80 was more unsaturated and mobile due to the presence of an alkyl chain with a double bond, an electron cloud, and the formation of transient polar functional groups. As a result, drug leakage increased and ultimately reduced the final entrapment efficiency (F4 vs. F3). In addition, it had a wider diameter than F3 and increased drug release in the Tween-80 formulation. Table 1 also shows the effect of surfactant type on liposome size. Based on the findings, the Tween-60 formulation had a smaller particle size than the Tween-80 formulation. This is because, compared to Tween-80, Tween-60 has the lowest HLB value.

Similar results have been reported by Nowroozi et al. [46] and Agarwal et al. [47]. They reported as the surfactant HLB values increase the hydrodynamic diameter of nanocarrier increase. The double bond of oleic acid in Tween-80 alters several physical properties relative to those of stearic acid in Tween-60. This double bond in the nanoliposome membrane results in looser packing in membranes and melting points and also enhancement in fluidity and permeability [48,49]. This phenomenon led to a significant drop in size, from 123.5 nm to 187.9 nm, was observed by replacing Tween-60 with Tween-80 and also increase and leakage of DOX from nanoliposome. DOPE is a neutral phospholipid with a cylindrical morphology and small head groups and prefers to form liposomal

(A)

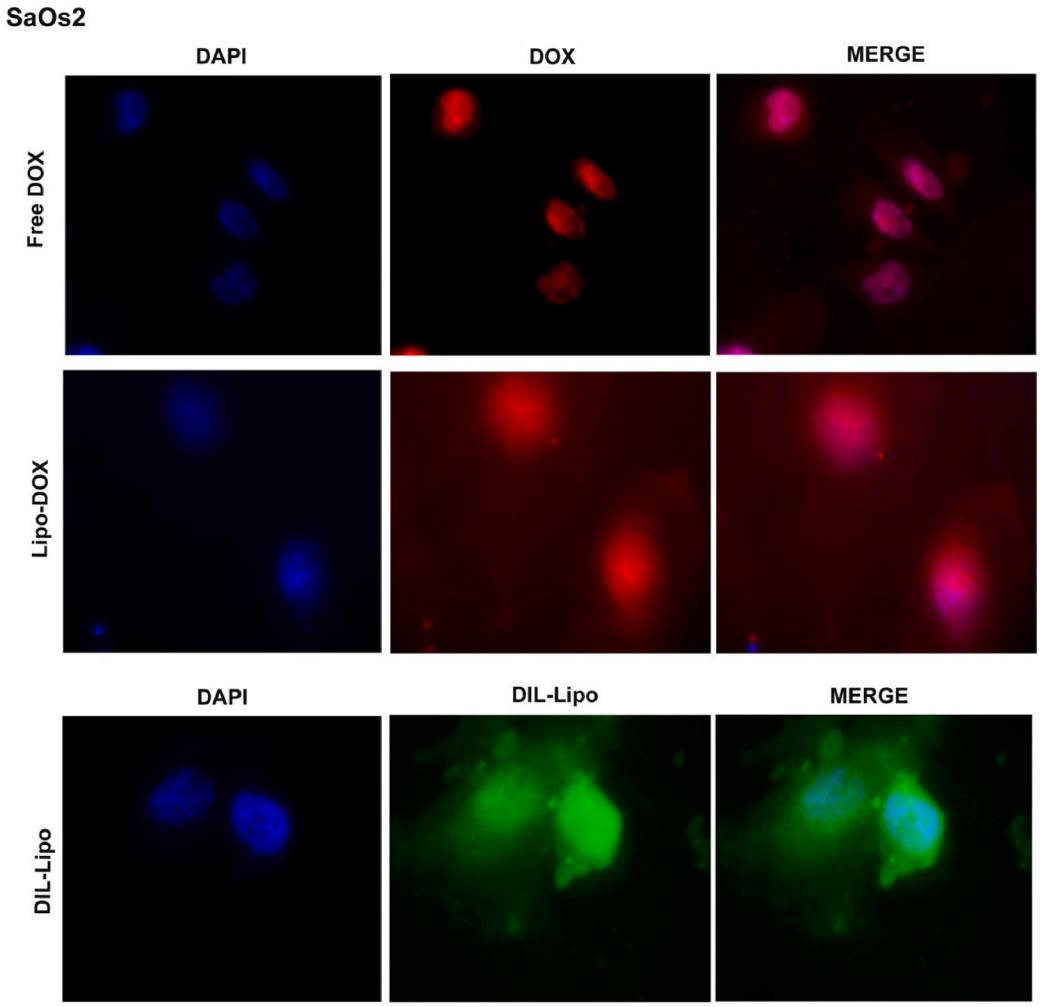

Fig. 8. Fluorescence microscopic images of cellular uptake of free DOX, Lipo-DOX, and blank liposomes in Saos-2 (A) and HFF cell lines (B).

spherical formations. Furthermore, the polar head of DOPE had poor hydration characteristics, which increased the hydrophobicity of liposomal bilayers and improved their fusion and contact with cellular membranes. This phenomenon demonstrates the presence of DOPE in liposomal structure can enhance cellular uptake and internalization of nanoliposomes [43]. Hence, 25% DOPE was added to the optimal formula. In this study, 5% DSPE-PEG2000 was added to the final formulation. Previous studies indicated that the addition of DSPE-PEG2000 enhances the stability of the liposomal drug, modifies the liposome surface, and promotes lamellar repulsion, leading to a decrease in the size and lamellarity of liposomes [50,51]. Pasut et al. fabricated super stealth liposomes (SSLs) using novel PEG-dendron-phospholipids to create liposomes with higher stability. They indicated the novel mPEG derivates in SSL increased stability and prolonged circulation half-life in comparison to the conventional stealth liposome. The mean size of all Dox-SSL formulations was less than 200 nm that it was consistent with our results [52]. Celia et al. demonstrated that PEGylation creates a steric barrier that prevents of aggregation nanoliposome and improves its stability [53]. PEGylation also results in the formation of liposomes with controlled release and less leakage [54]. The size of liposomes is an important parameter for stability in drug delivery systems [55]. A significant amount of the drug was loaded into the vesicles, which can be related to the proper ratios of cholesterol, phospholipid, Tween-60, polyethylene glycol, and drug, as well as the preparation method, according to the results of measuring the diameter of the liposome using DLS. The particle size of the liposome was confirmed to be 86.8 nm, and the drug encapsulation was found to be about 82%. The FTIR spectroscopy was performed to determine the chemical interaction between liposomes and DOX, as well as the interaction of DOX with the two-layer structure of liposomes. FTIR spectrum of liposome-containing DOX showed no new

(B)

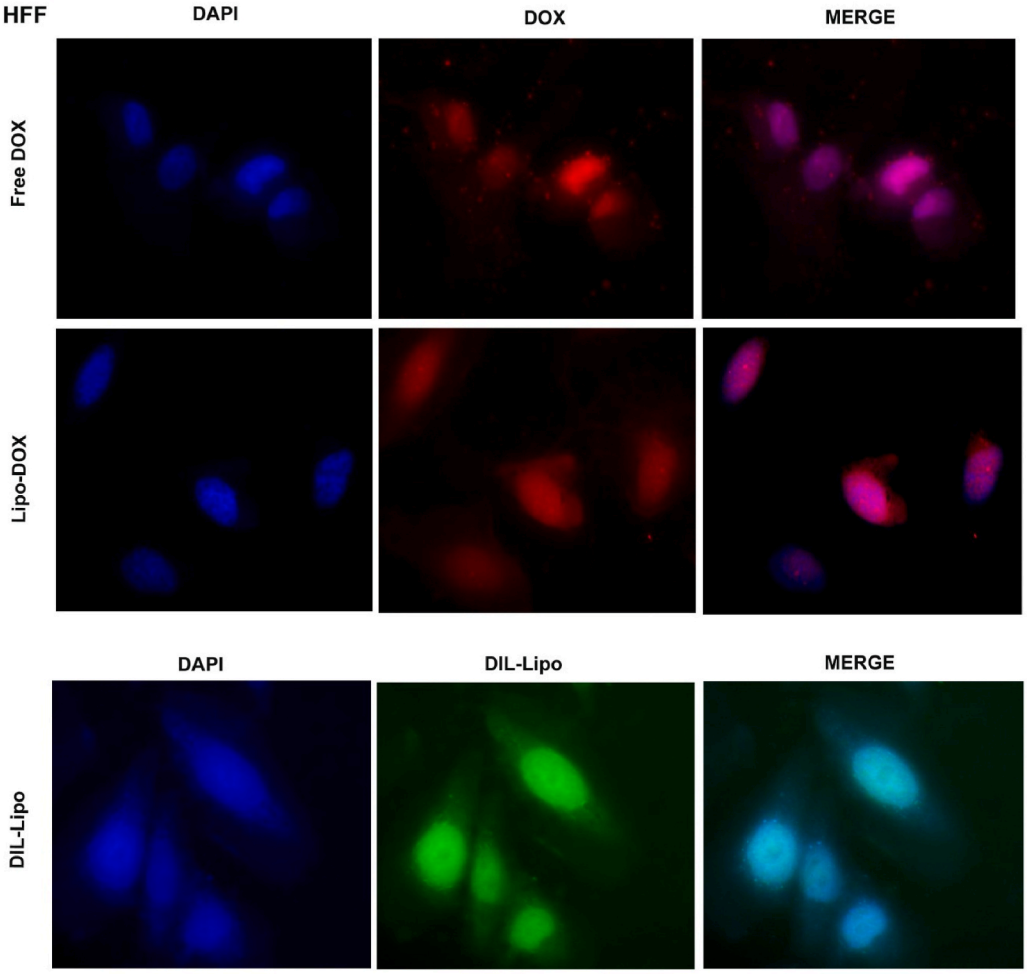

Fig. 8. (*continued*).

peak, and all peaks were repeated in blank liposome and Lipo-DOX, indicating no chemical interaction between the formulated system and DOX [56]. The results demonstrated that DOX in liposome form was stable during formulation. When the drug release pattern was examined for 72 h at 37 °C, it was discovered that the drug was released quite slowly, at a rate of roughly 30%. Also, in-vitro studies showed that the release of DOX from the nanoliposomal formulation is in two-phase patterns, with the initial rapid release of the drug in the first phase followed by the slower release of the drug in the second phase. The drug release test was also conducted at 42 °C to simulate drug release in tumor tissue conditions, which have a higher temperature because of its high mechanism. The findings demonstrated that higher temperatures resulted in quicker DOX release, demonstrating that PEGylated nanoliposomes are temperature sensitive. In a study performed by Sadat and colleagues, the effect of nanoliposomes containing DOX on osteosarcoma cell lines was investigated. Nanoliposomes were prepared using the pH gradient method, and the average diameter of nanoliposomes was 93 nm with a drug release rate of 46% after 48 h under acidic conditions. In our study, the drug release rate was about 30%, which indicates a significant reduction in drug release [57]. Also, Chantal Al-Sabbagh and colleagues [58] evaluated liposomal formulations containing fluorouracil in terms of temperature sensitivity and pharmacokinetic properties. They discovered significant drug release at 42 °C, supporting our findings that nanoliposomes are temperature sensitive. The MTT assay was employed to assess the cytotoxicity of liposomal DOX and the synthetic scaffold on osteosarcoma and HFF cell lines at various doses. Likewise, the cytotoxicity of the scaffold on HFF cells was evaluated for 1, 3, and 7 days. The findings showed that the alginate hydrogel scaffold had no cytotoxic effect on the HFF cells and instead boosted their growth rate over time. The findings of our investigation showed that the porous structure of the alginate hydrogel facilitated drug release and increased the toxicity of DOX on Saos-2 cancer cells, both in free and nanoliposomal forms, as compared to 2D cell culture. On cancer cell lines, the cytotoxic activity of nanoliposomal DOX was higher than that of free DOX, but doxorubicin-loaded nanoliposomes exhibited less toxicity on normal HFF cells. Our findings are consistent with previous

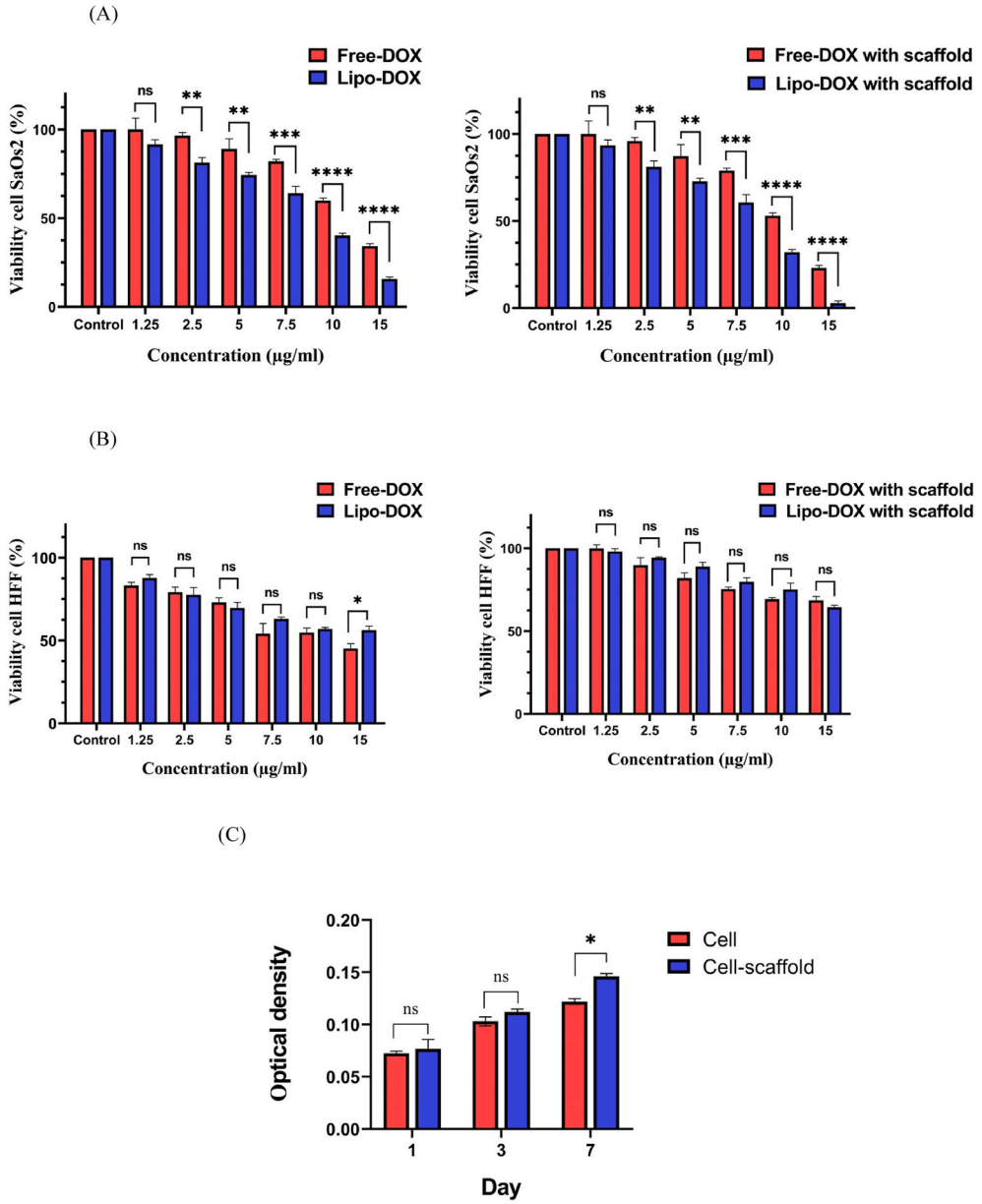

Fig. 9. The cytotoxicity assay of free DOX and Lipo-DOX on Saos-2 cell line (A) and HFF cell line (B) in 2D and 3D cell culture systems and sodium alginate scaffolds against HFF cell line (C); the values were expressed as mean ± SD of three independent experiments. *p < 0.05, **p < 0.01, ***p < 0.001, ****p < 0.0001.

research carried out in this field [59–62]. In addition, the 3D sodium alginate scaffold decreased the toxicity of DOX on HFF cells; similar findings were reported by Svanström et al. They established an Alginate-based 3D-printed scaffold as a tumor model for evaluating anti-cancer substances. As 3D scaffolds may simulate the microenvironment of cancer, anti-cancer medications such as DOX can have a stronger impact on malignant cells in 3D scaffolds than in conventional 2D cell culture [63], which is consistent with previous comparable studies [64,65]. Nanoliposomal DOX exhibits a higher fluorescence intensity than free DOX, as shown by the findings of cell uptake, which are in agreement with the MTT assay results. Lipo-DOX could penetrate cells more readily due to their nano-size and heat sensitivity [66–68].

5. Conclusion

This research aimed to develop a three-dimensional cell culture scaffold to provide an in-vitro environment for the Saos-2 cancer cell line that is comparable to the tumor microenvironment. This model aided in assessing and comparing the effectiveness and anti-

cancer mechanisms of chemotherapeutic agents in 2D and 3D culture systems, which could be a helpful platform to investigate cell behaviors and drug pharmacokinetic effects. Our findings demonstrated that the constructed scaffolds had the proper porosity and mechanical strength and had no influence on cell survival and proliferation. In order to assess the effectiveness of cancer in-vitro models, we examined the anti-tumor effects of DOX in both free and liposomal drug delivery systems in 2D and 3D cell culture systems. We developed a novel DOX-loaded PEGylated nanoliposome with a smaller size, higher entrapment efficiency, and sustained release pattern. These results show that the incorporation of DOX into nanoliposomes improves the pharmacokinetics of DOX and increases its cytotoxic effect against cancer cells. Lipo-DOX had a greater effect on malignant cells in 3D scaffolds than conventional 2D cell culture. Cancer cells were effectively seeded onto the 3D-based scaffold, which is an excellent alternative to the in-vivo cancer model, and this nano-delivery system is a potential technique to fight cancer cells.

Author contribution statement

Mastaneh Parchami: Performed the experiments; Wrote the paper.
Fateme Haghiralsadat: Conceived and designed the experiments.
Fatemeh Sadeghian-Nodoushan; Nasrin Ghasemi; Ghasem Sargazi: Analyzed and interpreted the data.
Mahdie Hemati: Conceived and designed the experiments; Contributed reagents, materials, analysis tools or data.
Sajjad Shahmohammadi: Performed the experiments.

Data availability statement

Data will be made available on request.

Declaration of interest's statement

The authors declare no conflict of interest.

Additional information

No additional information is available for this paper.

References

[1] Y.H. Jin-Peng He, Xiao-Lin Wang, Xiao-Jin Yang, Jing-Fan Shao, Feng-Jin Guo, Jie-Xiong Feng, Review of the Molecular Pathogenesis of Osteosarcoma, 2014.
[2] D. Osuna, E. de Álava, Molecular pathology of sarcomas, Rev. Recent Clin. Trials 4 (1) (2009) 12–26.
[3] G. Ottaviani, N. Jaffe, The Epidemiology of Osteosarcoma, Pediatric and Adolescent Osteosarcoma, 2009, pp. 3–13.
[4] J.W.V. de Azevedo, T.A. A.d.M. Fernandes, J.V. Fernandes, J.C.V. de Azevedo, D.C.F. Lanza, C.M. Bezerra, V.S. Andrade, J.M.G. de Araujo, Biology and pathogenesis of human osteosarcoma, Oncol. Lett. 19 (2) (2020) 1099–1116.
[5] Y. Zhang, J. Yang, N. Zhao, C. Wang, S. Kamar, Y. Zhou, Z. He, J. Yang, B. Sun, X. Shi, Progress in the chemotherapeutic treatment of osteosarcoma, Oncol. Lett. 16 (5) (2018) 6228–6237.
[6] M. Hemati, F. Haghiralsadat, F. Jafary, S. Moosavizadeh, A. Moradi, Targeting cell cycle protein in gastric cancer with CDC20siRNA and anticancer drugs (doxorubicin and quercetin) co-loaded cationic PEGylated nanoniosomes, Int. J. Nanomed. 14 (2019) 6575.
[7] D. Wang, X. Zhang, B. Xu, PEGylated doxorubicin prodrug-forming reduction-sensitive micelles with high drug loading and improved anticancer therapy, Front. Bioeng. Biotechnol. 9 (2021).
[8] O. Tacar, P. Sriamornsak, C.R. Dass, Doxorubicin: an update on anticancer molecular action, toxicity and novel drug delivery systems, J. Pharm. Pharmacol. 65 (2) (2013) 157–170.
[9] C.F. Thorn, C. Oshiro, S. Marsh, T. Hernandez-Boussard, H. McLeod, T.E. Klein, R.B. Altman, Doxorubicin pathways: pharmacodynamics and adverse effects, Pharmacogenetics Genom. 21 (7) (2011) 440.
[10] T. Hertiani, E. Sasmito, Ant plant (*Myrmecodia tuberosa*) hypocotyl extract modulates TCD4+ and TCD8+ cell profile of doxorubicin-induced immune-suppressed sprague dawley rats in vivo, Sci. Pharm. 81 (4) (2013) 1057–1070.
[11] S. Afereydoon, F. Haghiralsadat, N. Hamzian, A. Shams, M. Hemati, S.M. Naghib, M. Shabani, B. Zandieh-Doulabi, D. Tofighi, Multifunctional PEGylated niosomal nanoparticle-loaded herbal drugs as a novel nano-radiosensitizer and stimuli-sensitive nanocarrier for synergistic cancer therapy, Front. Bioeng. Biotechnol. 10 (2022).
[12] M. Çağdaş, A.D. Sezer, S. Bucak, Liposomes as potential drug carrier systems for drug delivery, Appl. Nanotechnol. Drug Deliv. 1 (2014) 1–50.
[13] M. Ghafari, F. Haghiralsadat, S. Khanamani Falahati-pour, J. Zavar Reza, Development of a novel liposomal nanoparticle formulation of cisplatin to breast cancer therapy, J. Cell. Biochem. 121 (7) (2020) 3584–3592.
[14] A. Fattahi Bafghi, B.F. Haghirosadat, F. Yazdian, F. Mirzaei, M. Pourmadadi, F. Pournasir, M. Hemati, S. Pournasir, A novel delivery of curcumin by the efficient nanoliposomal approach against Leishmania major, Prep. Biochem. Biotechnol. 51 (10) (2021) 990–997.
[15] H. Nsairat, D. Khater, U. Sayed, F. Odeh, A. Al Bawab, W. Alshaer, Liposomes: structure, composition, types, and clinical applications, Heliyon 8 (5) (2022), e09394.
[16] T. Helgason, T.S. Awad, K. Kristbergsson, E.A. Decker, D.J. McClements, J. Weiss, Impact of surfactant properties on oxidative stability of β-carotene encapsulated within solid lipid nanoparticles, J. Agric. Food Chem. 57 (17) (2009) 8033–8040.
[17] R. Kolašinac, C. Kleusch, T. Braun, R. Merkel, A. Csiszár, Deciphering the functional composition of fusogenic liposomes, Int. J. Mol. Sci. 19 (2) (2018) 346.
[18] L. Zhai, C. Luo, H. Gao, S. Du, J. Shi, F. Wang, A dual pH-responsive DOX-encapsulated liposome combined with glucose administration enhanced therapeutic efficacy of chemotherapy for cancer, Int. J. Nanomed. 16 (2021) 3185.
[19] J. Charmi, H. Nosrati, J.M. Amjad, R. Mohammadkhani, H. Danafar, Polyethylene glycol (PEG) decorated graphene oxide nanosheets for controlled release curcumin delivery, Heliyon 5 (4) (2019), e01466.
[20] S.R. Caliari, J.A. Burdick, A practical guide to hydrogels for cell culture, Nat. Methods 13 (5) (2016) 405–414.
[21] N. Sahu, D. Gupta, U. Nautiyal, Hydrogel: preparation, characterization and applications, Asian Pac. J. Nurs. Health Sci. 3 (1) (2020) 1–11.
[22] W. Wang, P. Zhang, W. Shan, J. Gao, W. Liang, A novel chitosan-based thermosensitive hydrogel containing doxorubicin liposomes for topical cancer therapy, J. Biomater. Sci. Polym. Ed. 24 (14) (2013) 1649–1659.

[23] R. Jadhav, A review on hydrogel as drug delivery system, World J. Pharmaceut. Res. 4 (2015) 578–599.
[24] E.M. Ahmed, Hydrogel: preparation, characterization, and applications: a review, J. Adv. Res. 6 (2) (2015) 105–121.
[25] E.M. Ahmed, Hydrogel: preparation, characterization, and applications: a review, J. Adv. Res. 6 (2) (2015) 105–121.
[26] K.Y. Lee, D.J. Mooney, Alginate: properties and biomedical applications, Prog. Polym. Sci. 37 (1) (2012) 106–126.
[27] M. George, T.E. Abraham, Polyionic hydrocolloids for the intestinal delivery of protein drugs: alginate and chitosan—a review, J. Contr. Release 114 (1) (2006) 1–14.
[28] S.N. Pawar, J. Edgar, Alginate derivatization: A review of chemistry, properties and applications, Biomaterials 33 (11) (2012).
[29] Pietro Matricardi, Interpenetrating Polymer Networks polysaccharide hydrogels for drug delivery and tissue engineering, Adv. Drug Deliv. Rev. 65 (9) (2013).
[30] A.R. Morais, N. Alencar Édo, F.H. Xavier Júnior, C.M. de Oliveira, H.R. Marcelino, G. Barratt, H. Fessi, E.S. do Egito, A. Elaissari, Freeze-drying of emulsified systems: a review, Int. J. Pharm. 503 (1–2) (2016) 102–114.
[31] Q.L. Loh, C. Choong, Three-dimensional scaffolds for tissue engineering applications: role of porosity and pore size, Tissue Eng. B Rev. 19 (6) (2013) 485–502.
[32] S.T. Tucci, A. Kheirolomoom, E.S. Ingham, L.M. Mahakian, S.M. Tam, J. Foiret, N.E. Hubbard, A.D. Borowsky, M. Baikoghli, R.H. Cheng, Tumor-specific delivery of gemcitabine with activatable liposomes, J. Contr. Release 309 (2019) 277–288.
[33] C. Bing, P. Patel, R.M. Staruch, S. Shaikh, J. Nofiele, M. Wodzak Staruch, D. Szczepanski, N.S. Williams, T. Laetsch, R. Chopra, Longer heating duration increases localized doxorubicin deposition and therapeutic index in Vx2 tumors using MR-HIFU mild hyperthermia and thermosensitive liposomal doxorubicin, Int. J. Hyperther. 36 (1) (2019) 195–202.
[34] Y. Xu, S. Long, Y. Yang, F. Zhou, N. Dong, K. Yan, B. Wang, Y. Zeng, N. Du, X. Li, Mathematical simulation of temperature distribution in tumor tissue and surrounding healthy tissue treated by laser combined with indocyanine green, Theor. Biol. Med. Model. 16 (1) (2019) 1–11.
[35] D. Kirui, C. Celia, R. Molinaro, S. Bansal, D. Cosco, M. Fresta, H. Shen, M. Ferrari, Mild hyperthermia enhances transport of liposomal gemcitabine and improves *in vivo* therapeutic response, Adv. Healthcare Mater. (2015) 4.
[36] M. Ravi, V. Paramesh, S. Kaviya, E. Anuradha, F.P. Solomon, 3D cell culture systems: advantages and applications, J. Cell. Physiol. 230 (1) (2015) 16–26.
[37] M. Zhang, X. Zhao, Alginate hydrogel dressings for advanced wound management, Int. J. Biol. Macromol. 162 (2020) 1414–1428.
[38] M. Qin, Y.E.K. Lee, A. Ray, R. Kopelman, Overcoming cancer multidrug resistance by codelivery of doxorubicin and verapamil with hydrogel nanoparticles, Macromol. Biosci. 14 (8) (2014) 1106–1115.
[39] M. Liu, X. Song, Y. Wen, J.-L. Zhu, J. Li, Injectable thermoresponsive hydrogel formed by alginate-g-poly (N-isopropylacrylamide) that releases doxorubicin-encapsulated micelles as a smart drug delivery system, ACS Appl. Mater. Interfaces 9 (41) (2017) 35673–35682.
[40] P. Nakhaei, R. Margiana, D.O. Bokov, W.K. Abdelbasset, M.A.J. Kouhbanani, R.S. Varma, F. Marofi, M. Jarahian, N. Beheshtkhoo, Liposomes: structure, biomedical applications, and stability parameters with emphasis on cholesterol, Front. Bioeng. Biotechnol. 9 (2021).
[41] M.L. Briuglia, C. Rotella, A. McFarlane, D.A. Lamprou, Influence of cholesterol on liposome stability and on in vitro drug release, Drug Deliv. Transl. Res. 5 (3) (2015) 231–242.
[42] Z. Sezgin-Bayindir, S. Losada-Barreiro, C. Bravo-Díaz, M. Sova, J. Kristl, L. Saso, Nanotechnology-based drug delivery to improve the therapeutic benefits of NRF2 modulators in cancer therapy, Antioxidants 10 (5) (2021) 685.
[43] J. Li, X. Wang, T. Zhang, C. Wang, Z. Huang, X. Luo, Y. Deng, A review on phospholipids and their main applications in drug delivery systems, Asian J. Pharm. Sci. 10 (2) (2015) 81–98.
[44] S. Taymouri, J. Varshosaz, Effect of different types of surfactants on the physical properties and stability of carvedilol nano-niosomes, Adv. Biomed. Res. (2016) 5.
[45] L. Basiri, G. Rajabzadeh, A. Bostan, Physicochemical properties and release behavior of Span 60/Tween 60 niosomes as vehicle for α-Tocopherol delivery, LWT 84 (2017) 471–478.
[46] F. Nowroozi, A. Almasi, J. Javidi, A. Haeri, S. Dadashzadeh, Effect of surfactant type, cholesterol content and various downsizing methods on the particle size of niosomes, Iran. J. Pharm. Res. (IJPR) 17 (Suppl2) (2018) 1–11.
[47] S. Agarwal, V. Bakshi, P. Vitta, A. Raghuram, N. Udupa, Effect of cholesterol content and surfactant HLB on vesicle properties of niosomes, Indian J. Pharmaceut. Sci. 66 (1) (2004) 121.
[48] G. Giacometti, M. Marini, K. Papadopoulos, C. Ferreri, C. Chatgilialoglu, trans-Double bond-containing liposomes as potential carriers for drug delivery, Molecules 22 (12) (2017) 2082.
[49] R. Kothencz, R. Nagy, L. Bartha, Determination of HLB values of some nonionic surfactants and their mixtures, Studia Universitatis Babes-Bolyai, Chemia 62 (4) (2017) 451–459.
[50] L. Shi, J. Zhang, M. Zhao, S. Tang, X. Cheng, W. Zhang, W. Li, X. Liu, H. Peng, Q. Wang, Effects of polyethylene glycol on the surface of nanoparticles for targeted drug delivery, Nanoscale 13 (24) (2021) 10748–10764.
[51] M. Ghaffari, S.M. Kalantar, M. Hemati, A. Dehghani Firoozabadi, A. Asri, A. Shams, S. Jafari Ghalekohneh, F. Haghiralsadat, Co-delivery of miRNA-15a and miRNA-16–1 using cationic PEGylated niosomes downregulates Bcl-2 and induces apoptosis in prostate cancer cells, Biotechnol. Lett. 43 (5) (2021) 981–994.
[52] G. Pasut, D. Paolino, C. Celia, A. Mero, A.S. Joseph, J. Wolfram, D. Cosco, O. Schiavon, H. Shen, M. Fresta, Polyethylene glycol (PEG)-dendron phospholipids as innovative constructs for the preparation of super stealth liposomes for anticancer therapy, J. Contr. Release 199 (2015) 106–113.
[53] C. Celia, M. Cristiano, F. Froiio, M. Di Francesco, N. d'Avanzo, L. Di Marzio, M. Fresta, Nanoliposomes as multidrug carrier of gemcitabine/paclitaxel for the effective treatment of metastatic breast cancer disease: a comparison with gemzar and taxol, Adv. Therapeut. 4 (2020).
[54] S.S. Nunes, R.S. Fernandes, C.H. Cavalcante, I. da Costa César, E.A. Leite, S.C.A. Lopes, A. Ferretti, D. Rubello, D.M. Townsend, M.C. de Oliveira, et al., Influence of PEG coating on the biodistribution and tumor accumulation of pH-sensitive liposomes, Drug Deliv. Transl. Res. 9 (1) (2019) 123–130.
[55] N. Heldt, M. Gauger, J. Zhao, G. Slack, J. Pietryka, Y. Li, Characterization of a polymer-stabilized liposome system, React. Funct. Polym. 48 (1–3) (2001) 181–191.
[56] N. Teymouri, A. Alizadeh, F. Haghiralsadat, M. Hemati, Evaluation of sublethal effects of abamectin nanoformulation on Tetranychus urticae Koch (Acari: tetranychidae): nanoliposomal versus nanoniosomal abamectin, Int. J. Trop. Insect Sci. (2022) 1–13.
[57] F. Haghiralsadat, G. Amoabediny, M.H. Sheikhha, B. Zandieh-doulabi, S. Naderinezhad, M.N. Helder, T. Forouzanfar, New liposomal doxorubicin nanoformulation for osteosarcoma: drug release kinetic study based on thermo and pH sensitivity, Chem. Biol. Drug Des. 90 (3) (2017) 368–379.
[58] C. Al Sabbagh, N. Tsapis, A. Novell, P. Calleja-Gonzalez, J.-M. Escoffre, A. Bouakaz, H. Chacun, S. Denis, J. Vergnaud, C. Gueutin, Formulation and pharmacokinetics of thermosensitive stealth® liposomes encapsulating 5-fluorouracil, Pharmaceut. Res. 32 (5) (2015) 1585–1603.
[59] L. Serpe, M. Guido, R. Canaparo, E. Muntoni, R. Cavalli, P. Panzanelli, C.D. Pepa, A. Bargoni, A. Mauro, M.R. Gasco, Intracellular accumulation and cytotoxicity of doxorubicin with different pharmaceutical formulations in human cancer cell lines, J. Nanosci. Nanotechnol. 6 (9–10) (2006) 3062–3069.
[60] B.F. Haghiralsadat, S. Naderinezhad, G. Amoabediny, F. Montazeri, B. Zandieh Doulabi, Evaluation of the effects of surface charge on cytotoxicity of liposomal Doxorubicin on bone cancer cell line (Osteosarcoma), Daneshvar Med. 25 (6) (2020) 19–26.
[61] A. Papagiannaros, S. Hatziantoniou, K. Dimas, G.T. Papaioannou, C. Demetzos, A liposomal formulation of doxorubicin, composed of hexadecylphosphocholine (HePC): physicochemical characterization and cytotoxic activity against human cancer cell lines, Biomed. Pharmacother. 60 (1) (2006) 36–42.
[62] M. Hemati, F. Haghiralsadat, F. Yazdian, F. Jafari, A. Moradi, Z. Malekpour-Dehkordi, Development and characterization of a novel cationic PEGylated niosome-encapsulated forms of doxorubicin, quercetin and siRNA for the treatment of cancer by using combination therapy, Artificial Cells, Nanomed. Biotechnol. 47 (1) (2019) 1295–1311.
[63] A. Svanström, J. Rosendahl, S. Salerno, M.C. Leiva, P. Gregersson, M. Berglin, Y. Bogestål, J. Lausmaa, A. Oko, G. Chinga-Carrasco, Optimized alginate-based 3D printed scaffolds as a model of patient derived breast cancer microenvironments in drug discovery, Biomed. Mater. 16 (4) (2021), 045046.
[64] K. Aranci, M. Uzun, S. Su, S. Cesur, S. Ulag, A. Amin, M.M. Guncu, B. Aksu, S. Kolayli, C.B. Ustundag, 3D propolis-sodium alginate scaffolds: influence on structural parameters, release mechanisms, cell cytotoxicity and antibacterial activity, Molecules 25 (21) (2020) 5082.
[65] M. Jalayeri, A. Pirnia, E.P. Najafabad, A.M. Varzi, M. Gholami, Evaluation of alginate hydrogel cytotoxicity on three-dimensional culture of type A spermatogonial stem cells, Int. J. Biol. Macromol. 95 (2017) 888–894.

[66] W.-l. Chen, F. Li, Y. Tang, J.-z. Li, Z.-q. Yuan, Y. Liu, X.-f. Zhou, C. Liu, X.-n. Zhang, Stepwise pH-responsive nanoparticles for enhanced cellular uptake and on-demand intracellular release of doxorubicin, Int. J. Nanomed. 12 (2017) 4241.
[67] H. Feng, D. Chu, Z. Li, Z. Guo, L. Jin, B. Fan, J. Zhang, J. Li, A DOX-loaded polymer micelle for effectively inhibiting cancer cells, RSC Adv. 8 (46) (2018) 25949–25954.
[68] F. Haghiralsadat, G. Amoabediny, M.H. Sheikhha, T. Forouzanfar, M.N. Helder, B. Zandieh-Doulabi, A novel approach on drug delivery: investigation of a new nano-formulation of liposomal doxorubicin and biological evaluation of entrapped doxorubicin on various osteosarcoma cell lines, Cell J. (Yakhteh). 19 (Suppl 1) (2017) 55.